applied sciences

MDPI

Article

Experimental Study on Mechanical Properties of Graded EPS–Steel Fiber-Reinforced Concrete

Yangsheng Wang * and Xinshan Zhuang

Hubei Provincial Ecological Road Engineering Technology Research Center, Hubei University of Technology, Wuhan 430068, China; zhuangxinshan@hbut.edu.cn
* Correspondence: 18162768813@163.com

Abstract: This study designs the aggregate gradation and calculates the benchmark mix proportion of concrete based on two sets of regression coefficients. Copper-plated micro-steel fibers and graded EPS (expanded polystyrene) particles, with varying volume ratios of cementing materials, were incorporated into concrete specimens of C30, C40, and C50 grades made from fine aggregates and gravel. The specimens underwent compressive strength, flexural strength, and slump tests to investigate and analyze the effects of steel fibers and graded EPS on the mechanical properties of concrete. A modified equation for the similar bending-to-compression ratio coefficient was established, and a method for calculating the extreme value of the similar bending-to-compression ratio under the combined action of graded EPS and steel fibers was proposed, in order to predict the optimal dosage of steel fibers and graded EPS. The results show that for concrete of all grades (fine aggregate and gravel groups), the compressive and bending failure modes exhibited high consistency. After incorporating EPS, the specimens displayed some ductility during compressive failure, and compressive strength was negatively correlated with the volume fraction of EPS. As the volume fraction of EPS increased, the workability of the concrete decreased. At 7 days of curing, the uniaxial compressive strength of the concrete specimens was 60–75% of the 28-day strength. The tensile failure of graded EPS–steel fiber concrete was divided into four stages. For every 0.25% increase in steel fiber volume fraction, the increase in flexural strength was most likely between 14.35% and 17.61%, with the maximum growth rate being approximately 27%, and the distribution of growth rates was relatively dispersed. When applying the current bending-to-compression ratio model to calculate the flexural strength of concrete under the combined action of graded EPS and steel fibers, a significant deviation from the experimental values was observed. By introducing the modified similar bending-to-compression ratio coefficient equation, a conversion relationship between compressive strength and flexural strength was established. The adjusted R-value was 0.989, and a comparison of the predicted values with the experimental results showed high accuracy, offering considerable reference value.

Keywords: mix proportion design; compressive strength; flexural strength; workability; modified similar bending-to-compression ratio coefficient equation

check for updates

Academic Editor: Asterios Bakolas

Received: 20 December 2024
Revised: 23 January 2025
Accepted: 2 February 2025
Published: 13 February 2025

Citation: Wang, Y.; Zhuang, X. Experimental Study on Mechanical Properties of Graded EPS–Steel Fiber-Reinforced Concrete. *Appl. Sci.* **2025**, *15*, 1980. https://doi.org/10.3390/app15041980

Copyright: © 2025 by the authors. Licensee MDPI, Basel, Switzerland. This article is an open access article distributed under the terms and conditions of the Creative Commons Attribution (CC BY) license (https://creativecommons.org/licenses/by/4.0/).

1. Introduction

In modern municipal engineering, facilities such as roads, reservoirs, and firewalls place high demands on the mechanical properties of concrete. With the advancement of technology, the performance requirements for concrete in practical engineering have risen significantly. A key focus of current research is to improve the mechanical properties

of concrete while minimizing its self-weight. This has become a major topic in the field today. EPS (expanded polystyrene) foam particles are a high-quality, eco-friendly building material that plays a significant role in enhancing the lightweight and thermal insulation properties of concrete. The use of EPS particles not only helps in reducing waste but also contributes positively to environmental management [1–3]. Research has shown that EPS foam particles can improve the water erosion resistance of concrete [4]. When EPS foam particles are used as admixtures to replace some of the components in concrete, the density of the concrete decreases, while its thermal insulation properties are enhanced, and its ability to buffer impact stress waves is significantly improved [5–7]. Srinivas et al. [8,9] incorporated 15% EPS particles into concrete, and their comparison revealed that this concrete mixture had a 24% reduction in weight compared with ordinary concrete. Patricia et al. [10] found that incorporating a certain volume fraction of EPS particles as aggregates into concrete reduced the material's thermal conductivity, thereby improving its insulation properties.

To achieve the goal of reducing the self-weight of concrete while improving its mechanical performance, researchers have also investigated the addition of fiber materials to concrete, in conjunction with EPS particles, to further enhance its mechanical properties. Yu, Z.P et al. [11] studied the effects of fabric fibers (polyester fibers, polypropylene mesh fibers, and polyacrylonitrile fibers) as admixtures. Luo Guoyi et al. [12–14] conducted an in-depth investigation into the mechanisms by which graphene oxide-grafted carbon fibers, polyvinyl alcohol (PVA) fibers, and basalt fibers modify the mechanical properties of concrete. Utilizing X-ray diffraction (XRD) and scanning electron microscopy (SEM) techniques, they systematically analyzed the permeability resistance of concrete incorporating these fibers. Their research elucidated the synergistic mechanisms between the microstructural characteristics and macroscopic performance of fiber-reinforced concrete. Their research demonstrated that polyester fibers can effectively improve the compressive strength, splitting tensile strength, and flexural strength of concrete. Li, Q.R et al. [15,16] proposed, through constitutive models and experiments, that the inclusion of steel fibers in concrete results in improved bending toughness and provided an evaluation method for this property. To address the segregation phenomenon caused by the significantly lower apparent density of EPS particles compared with the density of the cementing materials in concrete, previous studies have used epoxy resins or water-soluble ethylene–vinyl acetate copolymers as binders, effectively resolving this issue [17,18].

Although a considerable amount of research has been conducted on the relationship between EPS particles and the mechanical properties of concrete, most studies focus on the effects of EPS particles with a single particle size on the mechanical performance of concrete, typically using a single concrete grade and mix proportion for experimental investigations [19,20]. In practical engineering, however, the application scenarios of concrete are diverse, and different concrete grades in various locations and working conditions impose distinct requirements on aggregate particle size and gradation. As a result, experimental findings based on a single concrete grade and mix ratio are often difficult to generalize.

To address this issue, this study proposes an innovative experimental approach based on three commonly used concrete grades—C30, C40, and C50—incorporating aggregate gradation design and the optimization of the volume fraction of cementitious materials. The approach first involves the precise design of aggregate gradation for different concrete grades to optimize the concrete mix proportions. Next, a combination of EPS particles with varying volume fractions, copper-coated micro-steel fibers, and a small amount of epoxy resin is used to optimize the performance of the concrete. A series of tests, including flowability, compressive strength, and flexural strength tests, are conducted to investigate the combined effects of graded EPS particles, steel fibers, and epoxy resin on the mechanical

properties of concrete. Finally, a modified model based on the flexural-to-compressive strength ratio is employed to predict the flexural strength. This methodology not only offers a novel approach for enhancing the mechanical properties of multi-grade concrete but also provides a theoretical foundation for optimizing concrete mix designs in applications that require low-density, crack-resistant materials, such as in large-span structures of high-rise buildings and tunnel linings in subway systems.

2. Materials and Methods

2.1. Test Materials

In this experiment, P.O. 42.5 ordinary Portland cement with a density of 3.25 g/cm^3 and a specific surface area of 370 m^2/kg was used. The cement was supplied by Huaxin Cement (Huangshi, Hubei, China), and its chemical composition is shown in Table 1. The EPS (expanded polystyrene) foam particles have an apparent density of 0.035 g/cm^3, with particle sizes of 1 mm and 5 mm selected for the study. Copper-coated microfilament steel fibers, with a length of 12 mm and a single fiber diameter of 0.25 mm, were employed. These fibers have an elastic modulus of 214 GPa, a density of 7.76 g/cm^3, a maximum elongation of 25%, and a tensile strength of $\geq$2860 MPa. The appearance of the EPS particles and copper-coated microfilament steel fibers is shown in Figure 1. The coarse aggregates used were limestone fine aggregates and pebbles, while the fine aggregates consisted of either manufactured sand or natural sand. The fineness modulus of the manufactured sand was in the range of 2.4 to 2.8, while that of the natural sand was in the range of 2.3 to 3.0. The detailed parameters of the manufactured sand used in this experiment are provided in Table 2. A high-performance polycarboxylate superplasticizer (HT-100) (From Dalian oak Co., Ltd., Liaoning, China) was used as the water-reducing agent, with a recommended dosage of 1.5% and a water-reducing rate of 25%. The binder selected was a resin with a moderate epoxy value (0.25–0.45). The proportion of epoxy resin added in the experiment was (m_epoxy resin : m_aggregate = 0.05).

Table 1. The chemical composition of ordinary Portland cement is as follows.

Material Composition (%)	SiO_2	Al_2O_3	Fe_2O_3	CaO	MgO	SO_3
P.O 42.5	21.85	4.75	3.15	61.50	0.95	7.5



(**a**) (**b**)

Figure 1. Appearance of EPS particles and copper-coated microfiber steel fiber: (**a**) graded EPS; (**b**) copper-plated microfilament steel fiber.

Table 2. Related parameters of artificial sand.

Coarse-Grained Group 2~0.5 mm	Medium Particle Size Group 0.5~0.25 mm	Fine-Grained Group 0.25~0.075 mm	Uneven Coefficient Cu	Natural Moisture Content ω%
11.5	22.9	65.6	2.77	13.45

2.2. Experimental Plan

The design of the aggregate gradation is completed first to ensure the rationality of the selected concrete aggregates. Then, based on two sets of different regression coefficients, the mix proportions for the premixed C30, C40, and C50 grades of gravel and fine aggregate concrete are calculated. According to previous studies, improvements in the mechanical properties of concrete are most notable when the steel fiber volume fraction ranges from 1.5% to 2.25%, and the EPS (expanded polystyrene) volume fraction is between 10% and 30% [21–23]. In this study, the steel fiber and EPS volume fractions were expanded (1.5%, 1.75%, 2.25% and 15%, 25%, 35%) to set up experimental groups. EPS particles with particle sizes of 1 mm and 5 mm were selected [24], with each particle size occupying 50% of the total volume. The concrete preparation followed the guidelines outlined in the **"Premixed Concrete"** standard (GB/T14902-2012) [25]. The experiments were conducted according to the standards of **"Test Methods for the Mechanical Properties of Ordinary Concrete"** (GB/T50081-2019) [26] and **"Test Methods for Fiber Reinforced Concrete"** (CECS13-2009) [27].

For the compressive strength test, the specimens were 150 mm × 150 mm × 150 mm in size, and a uniform, continuous load was applied until the specimen failed. For the flexural toughness test, the specimens were 150 mm × 150 mm × 550 mm standard beams, tested using a 50–300 kN flexural test machine, applying a two-point load at the third-point location. The loading speed was maintained at 0.05 MPa/s to 0.08 MPa/s until failure. Based on the test results, the variations in compressive and flexural strengths of concrete incorporating steel fibers and graded EPS particles were analyzed.

2.3. Material Grading Curve

The significance of aggregate gradation design lies in the fact that the quality and gradation of aggregates have a critical impact on the performance of concrete. When aggregates contain excessive fine particles, it can lead to issues such as poor workability and the formation of cracks in the concrete. Inadequate gradation distribution can also negatively affect the consistency, strength, and durability of the concrete. Therefore, the rational selection of aggregates and the design of their gradation are crucial to ensuring the reliability of the experiment. In this study, the maximum aggregate particle size is 16 mm. According to the standards, the cumulative sieve passing percentage (%) and the individual sieve passing percentage (%) are calculated using the median value. The aggregate gradation is designed using a planning optimization method, and the detailed parameters are provided in Table 2. The aggregate gradation curve is shown in Figure 2.

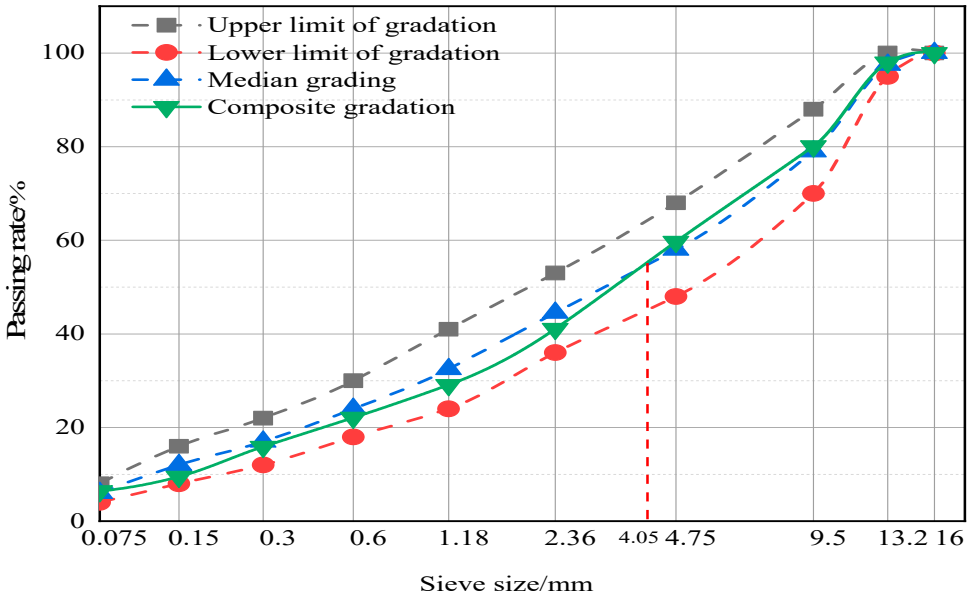


Figure 2. Grading curve of aggregates.

From the gradation curve, it can be observed that the combined gradation curve lies between the upper and lower limits of the gradation, meeting the basic design requirements. It is worth noting that the combined gradation curve does not perfectly coincide with the average gradation curve. When the sieve size of the aggregates is in the range of 4.05 mm to 16 mm, the combined gradation curve is positioned above the average gradation curve. In the range of 0.075 mm to 4.05 mm, the combined gradation curve is below the average gradation curve. However, the combined gradation curve closely overlaps with the median gradation curve, indicating that the gradation design is reasonable and close to the optimal state. The mineral proportions of the gradation curve are shown in Table 3.

Table 3. Aggregate grading parameters.

Nominal Particle Size (mm)	**Cumulative Sieve Residue on the Sieve (%)**										**Mineral Aggregate Proportion (%)**
	16	**13.2**	**9.5**	**4.75**	**2.36**	**1.18**	**0.6**	**0.3**	**0.15**	**0.075**	**35.6**
11–22	100	95.3	69.1	33.1	18.0	10.0	3.01	0.90	0.39	0.15	19.2
6–11	100	98.2	71.1	42.2	25.6	14.2	7.10	3.10	1.35	0.68	3.7
3–6	100	100	77.3	47.2	35.1	22.3	15.1	9.5	4.10	1.95	33.5
0.075–3	100	100	92.5	89.9	61.2	41.9	33.3	20.4	8.10	2.21	8.0
<0.075	100	100	100	100	100	100	99.7	98.4	77.5	56.5	/
Upper gradation limit	100	100	88	68	53	41	30	22	16	8	/
Lower gradation limit	100	95	70	48	36	24	18	12	8	4	/
Median gradation	100	97.5	79	58	44.5	32.5	24	17	12	6	/
Combined gradation	100	98.0	80.1	59.7	41.1	29.1	22.1	15.9	9.5	5.5	

The fluctuation of the combined gradation curve relative to the average gradation curve, as described above, suggests that the amount of aggregate with a particle size greater than 4.05 mm should be slightly lower than the corresponding value in the median gradation curve, while the amount of aggregate with a particle size smaller than 4.05 mm should be slightly higher than the corresponding value in the median gradation curve. Based on Horsfield's packing theory, the fluctuation phenomenon of the combined gradation curve can be explained as follows: The intersection point of the combined gradation curve and the median gradation curve occurs at 4.05 mm. In this experiment, 1 mm + 5 mm

graded EPS particles are incorporated into the aggregates. When the aggregate particle size exceeds 4.05 mm, the screening rate of the aggregates is increased, reducing the amount of aggregates larger than 4.05 mm, which is compensated by adding some 5 mm EPS particles. As a result, the combined gradation curve sinks, ensuring that it closely overlaps with the median gradation curve. When the EPS particles are added, the 5 mm EPS particles form a skeletal structure. By appropriately reducing the screening rate, the quantity of aggregates smaller than 1 mm is increased. This helps to fill the voids formed between the 5 mm EPS particles and the aggregates larger than 4.05 mm. As a result, the combined gradation curve rises and closely coincides with the median gradation curve, completing the optimal gradation design and forming the optimal skeletal-dense structure.

2.4. Mix Design

The experiment selected two sets of different regression coefficients to calculate the baseline mix proportions for C30, C40, and C50 fine aggregate concrete and gravel concrete. Then, the water-to-cement ratio of the baseline mix was increased and decreased, respectively, by 0.03 (maintaining the same water content while increasing or decreasing the cement content) to calculate two additional sets of mix proportions. Under the condition that the slump requirements were met, the concrete density correction factors were calculated. Subsequently, the 28-day compressive strength was used for strength validation, resulting in the optimal mix proportion for the laboratory, thus ensuring the rigor of the experiment. The parameters for the concrete mix calculation and the laboratory mix proportions are shown in Table 4.

Table 4. Calculation parameters of concrete mix proportions for each grade and optimal mix proportions in the laboratory.

Type	α_a	α_b	σ	β_s(%)	m_{co}	m_{wo}	m_{so}	m_{go}	Superplasticizer	δ(%)	W/C	Experimental Environment
					kg/m^3							
C30 gravel	0.49	0.13	5.0	28	318	147	542	1388	5	0.8	0.46	Class IIb
C30 fine aggregate	0.53	0.20	5.0	33	367	176	604	1228	5	0.5	0.48	
C40 gravel	0.49	0.13	5.0	29	349	150	561	1369	5	0.7	0.43	
C40 fine aggregate	0.53	0.20	5.0	35	368	169	643	1192	5	0.9	0.46	
C50 gravel	0.49	0.13	6.0	27	345	145	521	1408	5	0.7	0.42	
C50 fine aggregate	0.53	0.20	6.0	34	365	164	640	1230	5	0.6	0.45	

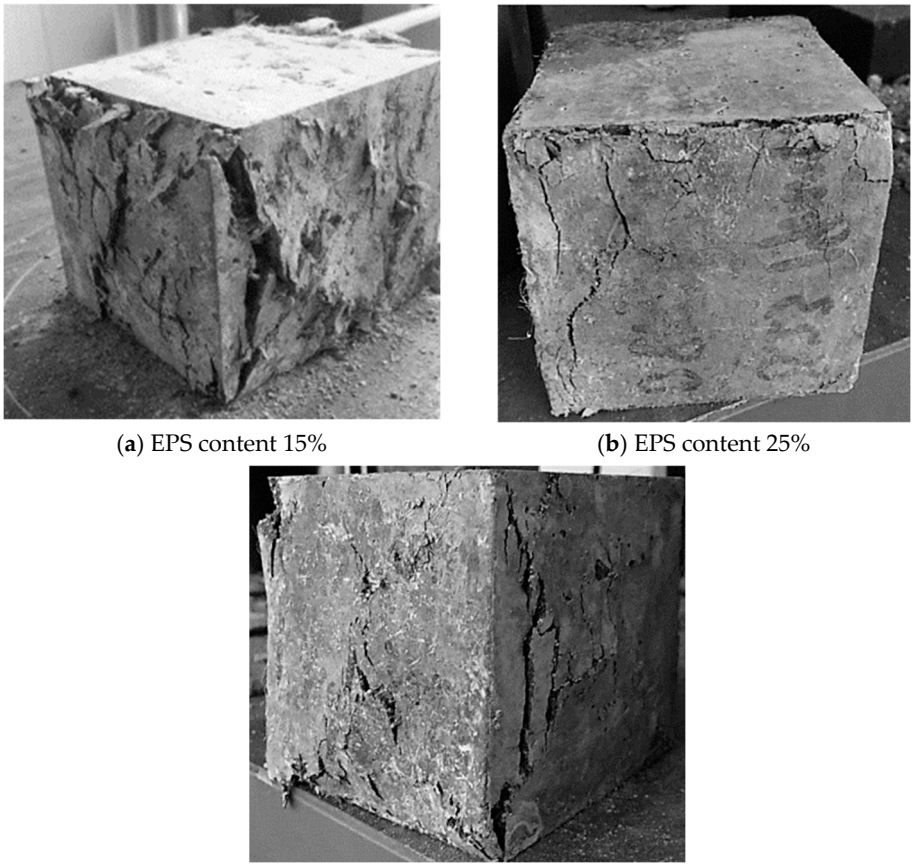
The experimental environment for this study is classified as Type IIb, where the maximum water-to-cement ratio is 0.50. The water-to-cement ratio design in Table 4 meets the required specifications. The correction factors in Table 4 are all less than 2%, indicating that this mix design is the optimal mix for the laboratory and does not require further adjustments.

3. Analysis of Experimental Phenomena and Results

3.1. Failure Mode of Compression Test Specimens

Due to the similar phenomena observed in the compressive strength tests of both gravel and fine aggregate concrete specimens at different concrete strength grades, the failure mode of the concrete containing a 1.75% volume fraction of steel fibers and graded EPS (expanded polystyrene) was selected for analysis, as shown in Figure 3. Overall, the specimens showed no large-scale fragment detachment after compression, due to the buffering effect of the EPS particles on energy absorption. The failure mode of the specimens shifted from the brittle failure typical of conventional concrete to a more ductile

failure. However, the failure pattern remained similar to that of ordinary concrete, with vertical, penetrating cracks propagating from top to bottom.



(**a**) EPS content 15% (**b**) EPS content 25%

(**c**) EPS content 35%

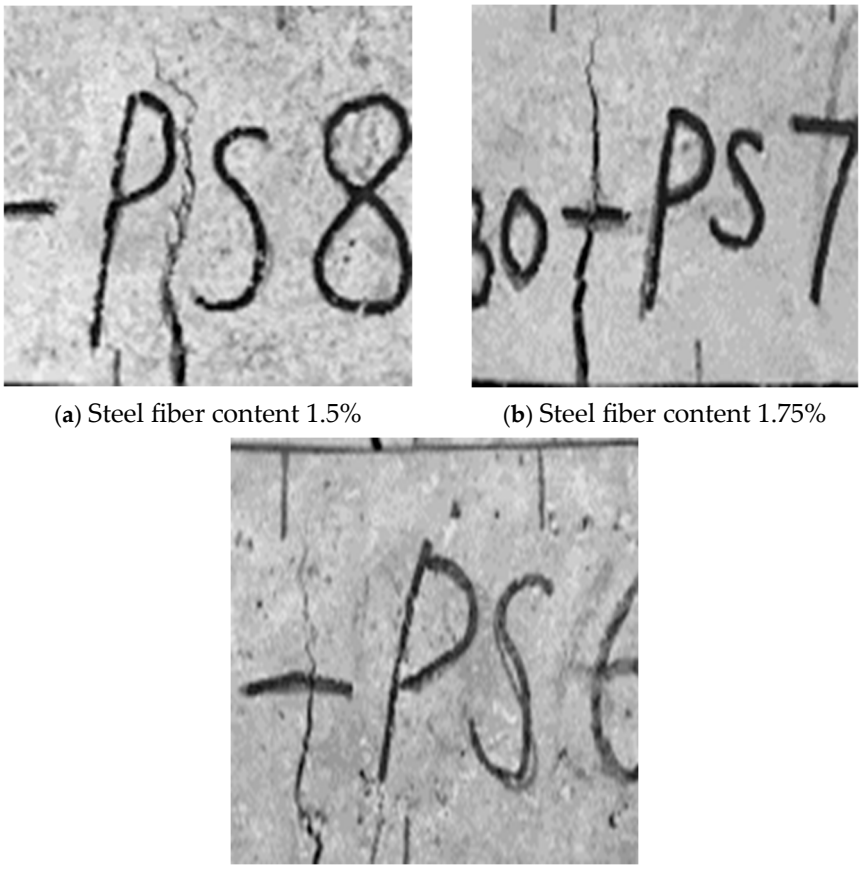
Figure 3. Compression failure mode of graded EPS–steel fiber-reinforced concrete specimens.

In Figure 3a, when the volume fraction of graded EPS was 15%, the specimens still tended towards brittle failure, exhibiting numerous wide penetrating cracks and larger volumes of unbroken fragments, with only slight ductility. As the volume fraction of graded EPS increased to 25%, the number and width of penetrating cracks significantly decreased, with most of the cracks being fine vertical, non-penetrating cracks, indicating improved ductility, as shown in Figure 3b. When the volume fraction of graded EPS increased to 35%, the replacement rate of aggregates with EPS particles was higher. At this stage, the EPS particles, with their strong hydrophobicity, failed to retain free water inside them, preventing adequate bonding with the cementitious materials. Additionally, the strength of the EPS particles was much lower than that of conventional aggregates, leading to the formation of wider penetrating cracks, though the number of cracks was fewer compared with the specimens with 15% graded EPS, as shown in Figure 3c.

3.2. Failure Mode of Flexural Test Specimen

As the results from the flexural tests of specimens with different volume fractions of graded EPS were essentially the same, the side failure modes of the flexural specimens containing 25% graded EPS at different steel fiber volume fractions were selected for reference, as shown in Figure 4. In general, the incorporation of steel fibers enhanced the bonding between the concrete aggregates. When small cracks formed due to loading, the steel fibers took on the main load. Additionally, due to the high tensile modulus of steel fibers, they effectively resisted the tensile stress generated at the crack faces, preventing

cracks from rapidly propagating from the bottom of the beam to the top. Therefore, the addition of steel fibers imparted a certain degree of ductility to the concrete during bending failure.



(**a**) Steel fiber content 1.5% (**b**) Steel fiber content 1.75%

(**c**) Steel fiber content 2.25%

Figure 4. Lateral cracks in the flexural test of graded EPS–steel fiber-reinforced concrete specimens.

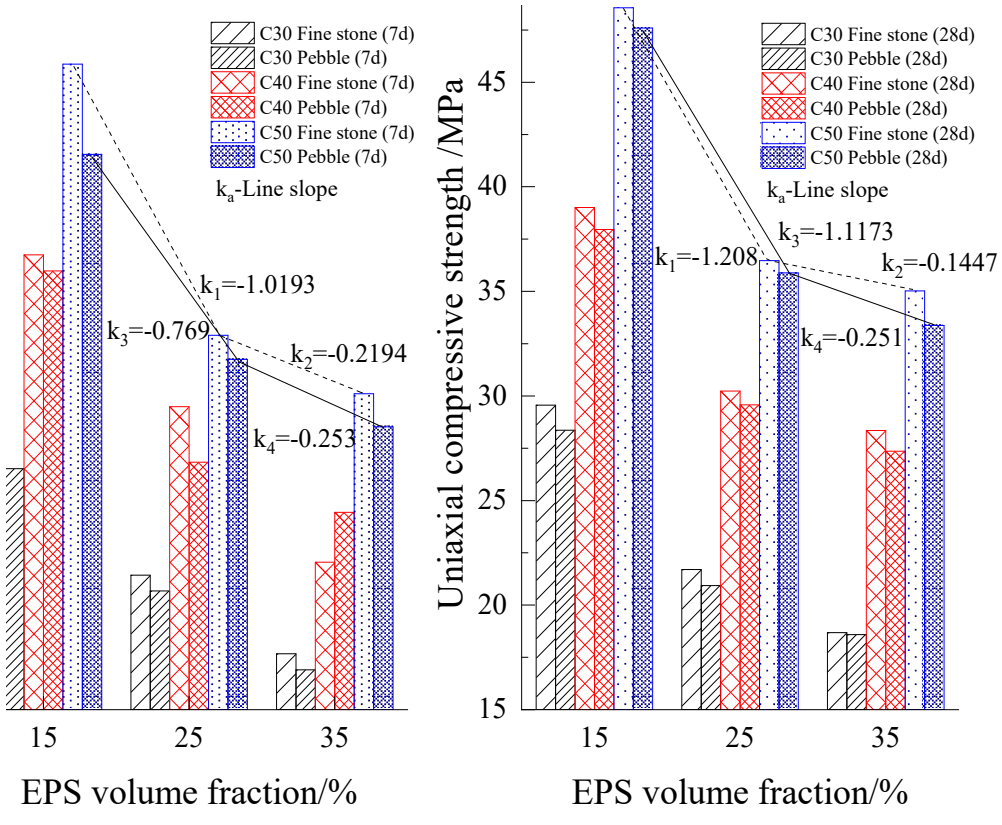
In Figure 4a, when the steel fiber volume fraction was 1.5%, the cracks at the bottom of the beam were wider, rougher, and rapidly extended toward the top of the beam. In Figure 4b, when the steel fiber volume fraction was 1.75%, the crack width at the bottom of the beam decreased, and although the crack still extended to the top, it appeared smoother, with no debris formation. There were only a few fine micro-cracks around the main crack. This phenomenon indicates that the bonding effect between the concrete aggregates was improved when the steel fiber volume fraction was 1.75%. In Figure 4c, when the steel fiber volume fraction increased to 2.25%, the cracks at the bottom of the beam extended to the centerline of the beam but did not propagate further to the top. No debris appeared, and no fine cracks were present around the main crack. Therefore, a steel fiber volume fraction of 2.25% provided the best bonding effect between the concrete aggregates.

3.3. Evaluation of Compressive Strength and Flowability

Figure 5 presents the relationship between the compressive strength of concrete at different ages and the volume fractions of steel fibers and graded EPS. The uniaxial compressive strength growth patterns of fine and gravel concrete with the incorporation of graded EPS and steel fibers at three different grades under standard curing at 7 and 28 days are generally similar. For example, in Figure 5a, the linear slope formed by the uniaxial compressive strength values of C50 fine (gravel) concrete at EPS volume fractions of 15%, 25%, and 35% at two different curing ages is demonstrated. In both 7-day and 28-day

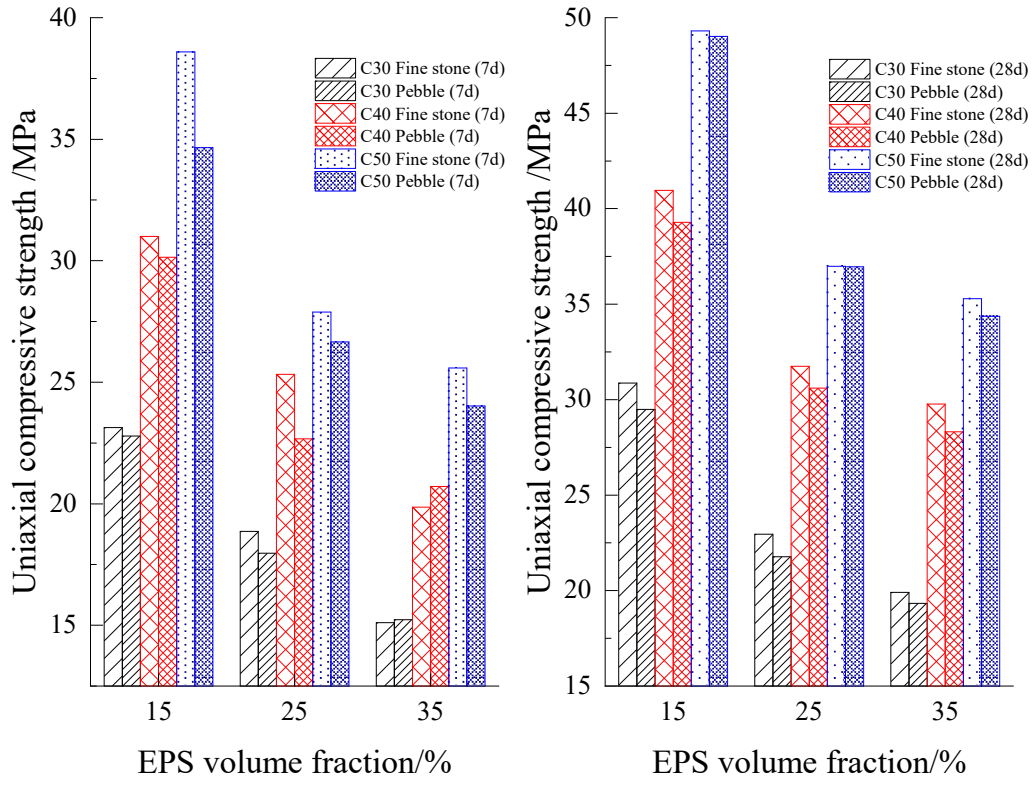
curing periods, the slopes are negative, with the absolute value of K_1 greater than that of K_2, and the absolute value of K_3 greater than that of K_4. This indicates that, with a constant steel fiber volume fraction, as the graded EPS volume fraction increases, the compressive strength of fine (gravel) concrete decreases at each curing age and grade. The reduction in compressive strength is more significant in the 15–25% EPS volume fraction range compared with the 25–35% range. The reactions observed in C30 and C40 concrete are similar to those in C50, so further discussion is omitted here.

The compressive modulus of EPS is much lower than that of concrete, which leads to a reduction in the uniaxial compressive strength of concrete when EPS is added. To explain the slowed rate of compressive strength reduction, the Weymouth particle interference theory [28] is applied. In the experimental concrete, the skeleton formed by coarse aggregates with a nominal particle size greater than 4.75 mm (specifically greater than 5 mm) is filled by finer aggregates and 5 mm EPS particles. The skeleton formed by fine aggregates with a nominal particle size less than 2.36 mm (specifically 2.36 mm to 1.18 mm) is filled by 1 mm EPS particles and mineral powders smaller than 0.075 mm. Additionally, since the designed aggregates are continuously graded, particles of each size are included, ensuring that each skeletal pore is filled with next-level aggregates smaller than the pore size. This process continues until the concrete reaches a dense state. The framework-dense structure, formed by coarse and fine aggregates, graded EPS particles, mineral powder, and cement, is considered an ideal configuration. When the EPS volume fraction increases from 25% to 35%, the filling effect is more pronounced than in the 15–25% range, which slows down the rate of compressive strength reduction.

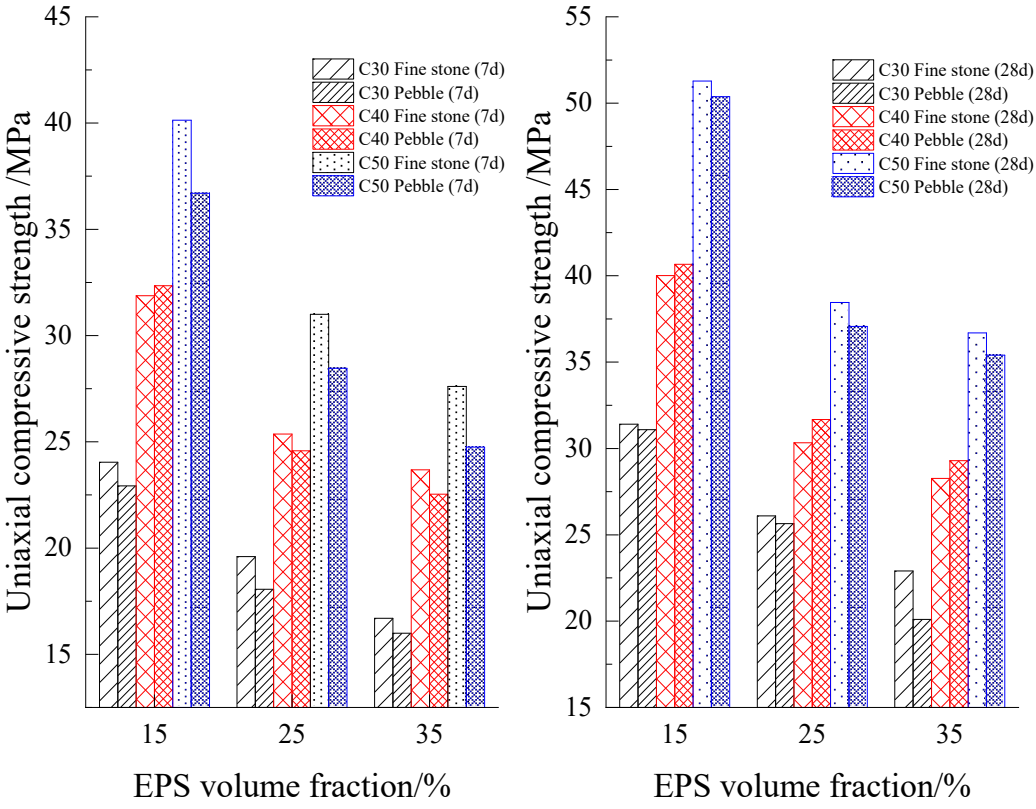


(**a**)

Figure 5. *Cont.*



(**b**)



(**c**)

Figure 5. Compressive strength of EPS–steel fiber-reinforced concrete with different age grades. (**a**) Uniaxial compressive strength of steel fibers with a volume fraction of 1.5% at different ages and EPS volumes. (**b**) Uniaxial compressive strength of steel fibers with a volume fraction of 1.75% at different ages and EPS volumes. (**c**) Uniaxial compressive strength of steel fibers with a volume fraction of 2.25% at different ages and EPS volumes.

By comparing the uniaxial compressive strength values of fine (gravel) concrete at 7 and 28 days for the same EPS and steel fiber volume fractions in Figure 5, it is found that the 7-day compressive strength reaches 60–75% of the 28-day value. This indicates that curing during the first 7 days is a crucial factor influencing the uniaxial compressive strength of concrete. Longitudinal comparisons of Figure 5a–c, corresponding to the same EPS volume fraction, show that increasing the steel fiber volume fraction leads to a slight increase in compressive strength, though the effect is not significant. For every 0.25% increase in steel fiber volume fraction, the increase in compressive strength is within 5%. Cracks form in the concrete due to internal stress concentrations, with fine cracks appearing at the mortar–aggregate interface. Steel fibers, distributed parallel to the aggregate boundaries, create a wall effect that provides a slight lateral restraint on crack propagation. As stress continues to increase, the internal cracks in the concrete lead to failure, extending into the hardened cement paste. Steel fibers then act as a reinforcement, slowing the rate of crack propagation, resulting in a small increase in compressive strength.

It is worth noting that in Figure 5c, at the 28-day standard curing age, all grades of fine (gravel) concrete specimens with a steel fiber volume fraction of 2.25% and EPS volume fraction of 15% achieve the standard compressive strength of concrete. This indicates that, under these proportions, graded EPS–steel fiber concrete can be directly selected for practical engineering without the need to increase the grade. For other combinations of steel fiber and EPS volume fractions, based on actual engineering requirements for compressive strength, the concrete grade may need to be increased by one to two grades to meet the design specifications.

The Standard for Testing Methods of Performance of Concrete Mixes, GB/T 50080–2002, stipulates that the slump and slump flow values of concrete mixtures are measured in millimeters, with precision to 1 mm and the result rounded to the nearest 5 mm [29]. Since the influence of steel fiber volume fractions of 1.5% and 2.25% on the slump of concrete, after rounding, is consistent with the value for a volume fraction of 1.75%, a steel fiber volume fraction of 1.75% was selected as the representative. The study investigates the effect of different gradation EPS volume fractions on the flowability of concrete. For a steel fiber volume fraction of 1.75%, the slump values of concrete corresponding to different gradation EPS volume fractions in the gravel and crushed stone groups are shown in Figure 6. Overall, the increase in gradation EPS volume fraction is negatively correlated with the flowability of concrete, and the slump decreases at an accelerating rate. In Figure 6a for fine aggregate concrete, when the EPS volume fraction increases from 15% to 25%, the slump of all three concrete grades decreases by 10 mm. When the EPS volume fraction continues to increase to 35%, the slump decreases by 20 mm for all three grades. In Figure 6b, for gravel aggregate concrete, when the EPS volume fraction increases from 15% to 25%, the slump of C30 and C40 concrete decreases by 10 mm, while that of C50 decreases by 5 mm. However, when the EPS volume fraction increases from 25% to 35%, the slump of C50 decreases by 20 mm, while the slump reduction for the other grades is 15 mm.

The influence of steel fibers and graded EPS on concrete flowability can be attributed to four main reasons:

1. **Aggregate replacement:** The 5 mm particles in graded EPS replace some coarse aggregates, and the 1 mm particles replace part of the fine aggregates. This improves the embedding effect of the concrete matrix structure, increases frictional resistance, and, at the same time, the lower density of EPS particles compared with aggregates reduces the vertical and diagonal component forces from the weight of the concrete matrix during the slump test, leading to a decrease in the slump (positive effect).

2. **Reduced water content:** the incorporation of graded EPS reduces the amount of water required for concrete [30], increasing the consistency and reducing the slump (positive effect).
3. **Hydrophobic nature of EPS particles:** EPS particles are hydrophobic, preventing the retention of free water on their surfaces. As a result, there is no liquid bridge connection between EPS particles and fine aggregate particles. According to the Young–Laplace theory, the absence of capillary suction between the two types of particles leads to an increase in the concrete slump (negative effect).
4. **Steel fiber length:** The length of steel fibers is much greater than the diameter of the aggregates. When steel fibers are incorporated, they consume more cement paste to surround them. Additionally, steel fibers may anchor the matrix, improving particle integrity and reducing the concrete slump (positive effect).

Based on these four influencing factors, the addition of graded EPS particles and steel fibers results in a macro response of reduced slump and decreased flowability of concrete.

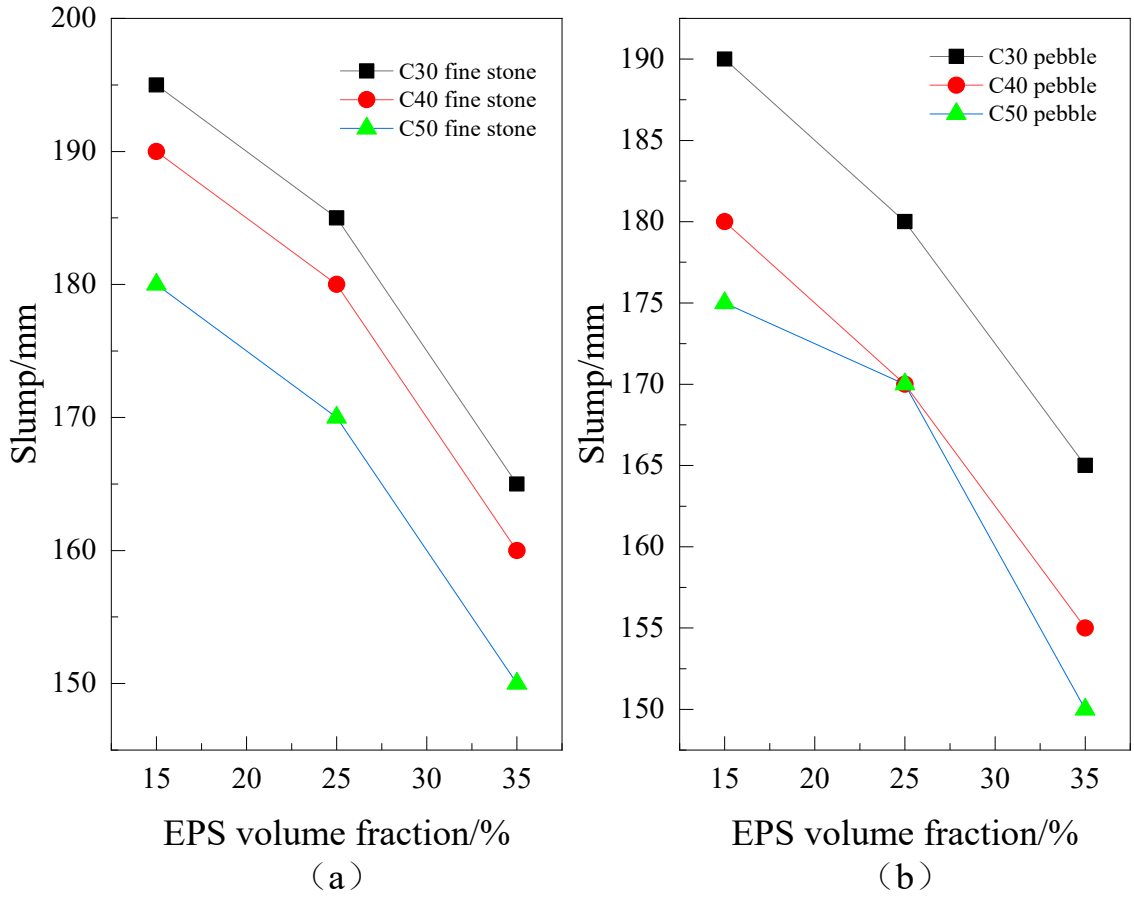


Figure 6. The effect of graded EPS volume fraction on the fluidity of concrete.

3.4. Flexural Strength and Failure Mechanism

The specimen will experience four distinct stages of deformation as the applied stress changes, As shown in Figure 7: the overall working stage (elastic deformation), crack development stage, steel fiber-dominated working stage (significant crack development), and specimen rupture (ductile failure). In the initial stage of loading, the specimen remains in the linear elastic phase. As the three-point loading gradually increases, the stress rises rapidly, and the specimen remains in the elastic phase, where the deformation can recover upon unloading (OA segment). However, as the stress increases quickly to 50–60% of the peak value at point A, small vertical cracks will appear inside the specimen, with no

external visible damage. At this point, the skeleton structure made up of coarse aggregates, fine aggregates, cement, and other materials is under stress. As the tensile stress continues to increase, the EPS and aggregates inside the skeleton are compressed and experience some damage. However, since EPS has good elasticity, the specimen only experiences minor plastic deformation, and fine cracks develop at the bottom.

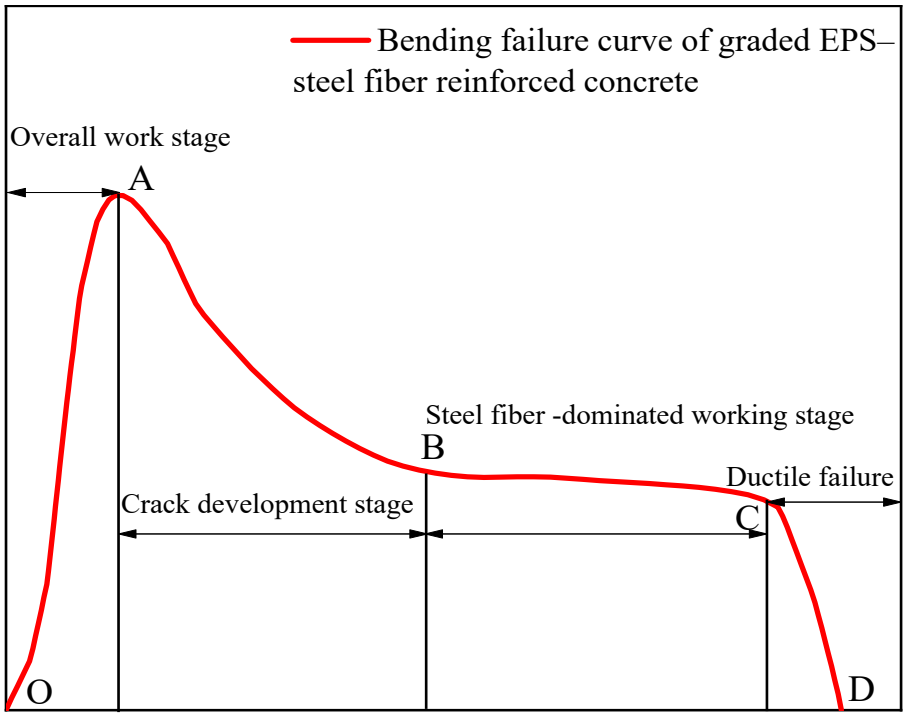


Figure 7. Graded EPS–steel fiber-reinforced concrete bending failure stage.

As the stress continues to increase to a peak at point A, the specimen formally enters the crack development stage. The tensile stress generated by the external load exceeds the load-bearing capacity of the skeleton structure. The neutral axis quickly moves upward, and the bottom of the specimen is pulled apart. Developmental cracks emerge and rapidly extend toward the top of the specimen. At this stage, the skeleton structure still dominates the load-bearing capacity, and steel fibers begin to participate in load-bearing (AB segment).

When the strain reaches point B, the cracks at the bottom of the specimen continue to develop. Several smaller micro-cracks appear adjacent to the main crack. As the deformation continues to increase, the main crack extends toward the top of the specimen. From point B onward, the steel fibers play a dominant role in bearing the tensile stress, thereby slowing the rate of development of the micro-cracks (BC segment).

As the strain increases to point C, the tensile stress in the specimen suddenly changes. At this point, the main crack width rapidly increases and extends to the top of the specimen. The specimen is about to rupture completely. However, due to the effect of the steel fibers, the failure is not linear (CD segment), indicating that the failure has a certain degree of ductility.

Based on the load-deflection curves of concrete with different gradations of EPS and steel fiber volume fractions, as shown in Figure 8, it can be observed that for the same grade, fine aggregate concrete reaches the peak stress in the elastic–plastic deformation phase earlier than gravel concrete, and the peak stress is also slightly higher. Additionally, high-grade concrete reaches the peak stress at a larger strain compared with low-grade concrete.

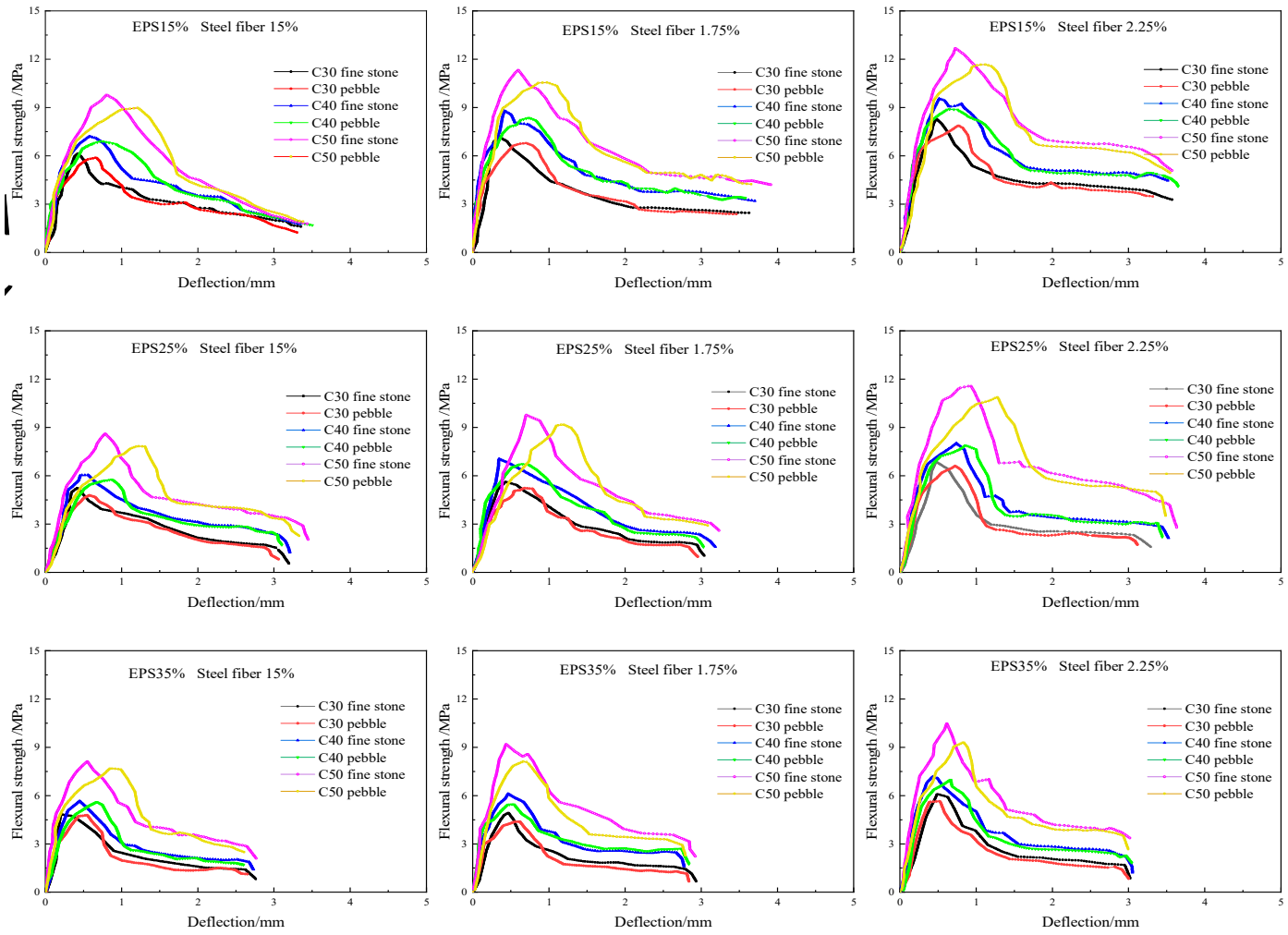


Figure 8. Load-deflection curve of graded EPS–steel fiber-reinforced concrete.

Overall, for all three EPS volume fractions, the flexural strength of each concrete grade increases as the steel fiber volume fraction increases from 1.5% to 2.25%. The change in steel fiber volume fraction has a minimal impact on the deflection value at the inflection point A during both the overall working stage (OA segment) and the crack development stage (AB segment). The deflection values at point A for all load-deflection curves fall within the range of (0.48, 1.12) mm, with the exception of the C50 gravel group, where the deflection at point A exceeds 1 mm. The A points for the other grades are more concentrated.

The steel fiber volume fraction is negatively correlated with the deflection value at point B, meaning that as the fiber content increases, the deflection value at point B decreases. However, the steel fiber volume fraction is positively correlated with the length of the BC segment. As a result, the deflection value at the critical failure point C increases, indicating an enhanced ability to resist failure.

The deflection values at point A for each grade of specimen are fairly concentrated, suggesting that changes in the steel fiber volume fraction have little effect on the specimen's response to tensile stress during the initial bending stage. Therefore, this change does not significantly impact the deflection values. The increase in steel fiber volume fraction leads to a reduction in the deflection value at point B. This occurs because, in the crack development stage, as the steel fiber volume fraction increases, the specimen begins to bear tensile stress earlier and enters the steel fiber-dominated working stage. Due to the excellent tensile properties of the steel fibers, the length of the BC segment increases, and the deflection value at the failure point C increases accordingly.

Table 5 presents the stress peak values and growth rates for concrete with different volume fractions of graded EPS and steel fiber content. It is observed that the stress peak values for all grades of graded EPS–steel fiber concrete are higher than those for the corresponding plain concrete of the same grade [31], indicating a positive enhancement effect.

Table 5. Peak stress and growth rate of concrete of different grades under different volume fractions.

EPS (%)	Steel Fiber (%)	Stress Peak Value (MPa)						Growth Rate (%)					
		C30A	C30a	C40B	C40b	C50C	C50c	A	a	B	b	C	c
15	1.5	6.18	5.86	7.19	6.89	9.75	8.97	/	/	/	/	/	/
	1.75	7.08	6.80	8.87	8.65	11.31	10.54	14.53	16.01	23.32	25.48	15.99	17.48
	2.25	8.30	7.87	9.61	8.87	12.66	11.67	17.25	15.66	8.33	2.55	11.93	10.74
25	1.5	5.21	4.73	6.04	5.74	8.58	7.80	/	/	/	/	/	/
	1.75	5.53	5.19	7.03	6.70	9.75	9.16	6.23	9.89	16.33	17.39	13.71	17.38
	2.25	6.85	6.59	8.01	7.87	11.55	10.86	23.92	26.83	13.9	17.46	18.36	18.64
35	1.5	4.79	4.37	5.65	5.41	8.10	7.64	/	/	/	/	/	/
	1.75	4.90	4.76	6.11	5.59	9.15	8.08	2.43	8.89	8.21	8.40	12.91	5.75
	2.25	6.04	5.64	7.23	6.97	10.45	9.28	23.21	18.51	18.3	24.66	14.25	14.81

Note: "A" represents fine aggregate, and "a" represents the gravel group; the same applies for the others.

For an EPS volume fraction of 15%, the growth rate of the flexural strength stress peak for both fine and coarse aggregate concrete lies within the range of (2.55%, 23.32%). At an EPS volume fraction of 25%, the growth rate falls within the range of (6.23%, 26.83%), while at an EPS volume fraction of 35%, it ranges from (2.43%, 24.66%). The standard deviations for each of these intervals are 6.178, 5.524, and 6.923, respectively, with coefficients of variation of 0.413, 0.331, and 0.518. To eliminate outliers, values falling below two standard deviations were discarded for each interval (the lower limit of each interval). After this adjustment, the average growth rates for the peak stress values corresponding to different steel fiber volume fractions under each of the three EPS volume fractions were found to be 16.06%, 17.61%, and 14.35%, respectively. These average values all fall within the 95% confidence interval.

From these data, it can be concluded that for every 0.25% increase in the steel fiber volume fraction, the enhancement in flexural strength is most likely to fall within the range of (14.35%, 17.61%). However, the maximum growth rate is approximately 27%, with a relatively wide distribution of growth rates. This indicates that the distribution of the steel fibers has a significant impact on the improvement of flexural performance.

3.5. Conversion Formula and Accuracy of Compression Ratio

There are few existing formulas for calculating the bending strength of graded EPS–fiber-reinforced concrete. Based on the bending strength calculation formula for ordinary concrete, combined with the formula for calculating the bending strength of recycled aggregate graded concrete proposed by Xiao Jianzhuang [32], the ($f_f = 0.75\sqrt{f_{cu}}$) formula was used to predict the bending strength of graded EPS–steel fiber concrete in this study. It was found that the predicted values showed significant deviation from the experimental values. The reason for this discrepancy lies in the differences in aggregates and grading, which cause substantial variations in the concrete skeleton structure, leading to a reduced accuracy of the formula. As a result, the prediction formula is no longer effective for estimating the bending strength of graded EPS–steel fiber concrete.

Considering that analyzing graded EPS or steel fibers in isolation cannot accurately predict the impact of their coupling on the bending-to-compression ratio of concrete, a coefficient equation ($f(\alpha, \beta)$) was introduced. Using the experimental data from this study,

the average values of the bending-to-compression ratios corresponding to the gravel group and fine aggregate group were taken as shown in Figure 9. The variation range of the class bending-to-compression ratio [33] ($f_f/\sqrt{f_{cu}}$) values is within 20%, and merging the data to calculate the average value has minimal impact on the deviation of the results. Through regression analysis, the formula coefficients for the bending-to-compression ratio under the coupled effect of graded EPS and steel fibers were adjusted.

$$f_f = \gamma(\alpha, \beta)\sqrt{f_{cu}} \quad (1)$$

$$\gamma(\alpha, \beta) = A + A_1\alpha + A_2\beta + A_3\alpha^2 + A_4\beta^2 + A_5\alpha\beta\text{—Correction coefficient formula} \quad (2)$$

The value of α ranges from 1.5 to 2.25, and the value of β ranges from 15 to 35.

In the equation, α represents the steel fiber volume fraction, β represents the graded EPS volume fraction, and A, A_1, A_2, A_3, A_4, A_5 is the variable control parameter. The formula for the concrete-like bending-to-compression ratio under the coupling effect of graded EPS and steel fibers is derived through fitting. The resulting formula coefficients are as shown in Equation (2) $\gamma(\alpha, \beta) = 2.56 - 1.4\alpha + 0.0045\beta + 0.4\alpha^2 + 7.68\beta^2 - 0.012\alpha\beta$. The adjusted RRR value is 0.989, The numerical accuracy of the test values and the prediction model in this paper is shown in Figure 10, indicating a good fit.

After deriving the specific control parameters, Equation (2) is substituted back into Equation (1) to obtain the modified formula for the flexural strength of graded EPS–steel fiber concrete, which is then validated using the compressive strength test values. By substituting $\frac{\partial\gamma(\alpha,\beta)}{\partial\alpha} = 0$ and $\frac{\partial\gamma(\alpha,\beta)}{\partial\beta} = 0$ from Equation (2), the maximum bending-to-compression ratio under the combined effect of graded EPS and steel fibers can be calculated, allowing for the prediction of the optimal volume fraction.

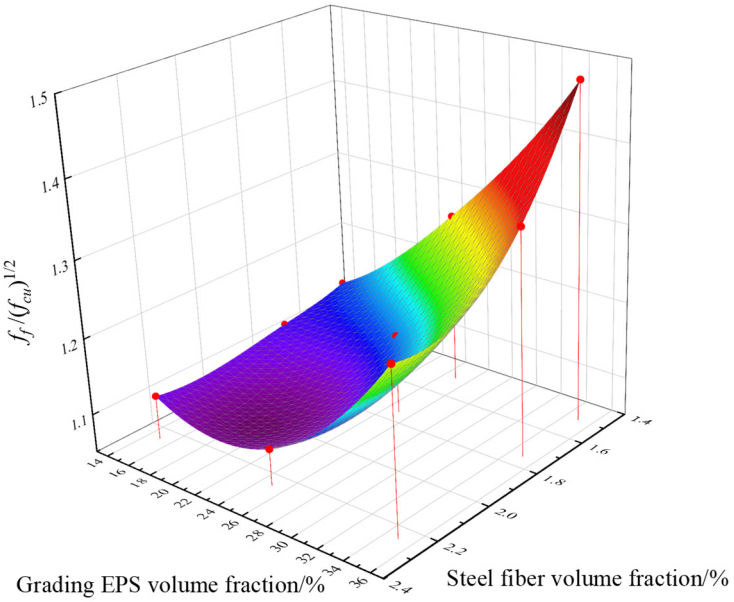


Figure 9. Curve fitting of flexural compression ratio under the coupling effect of graded EPS and steel fibers.

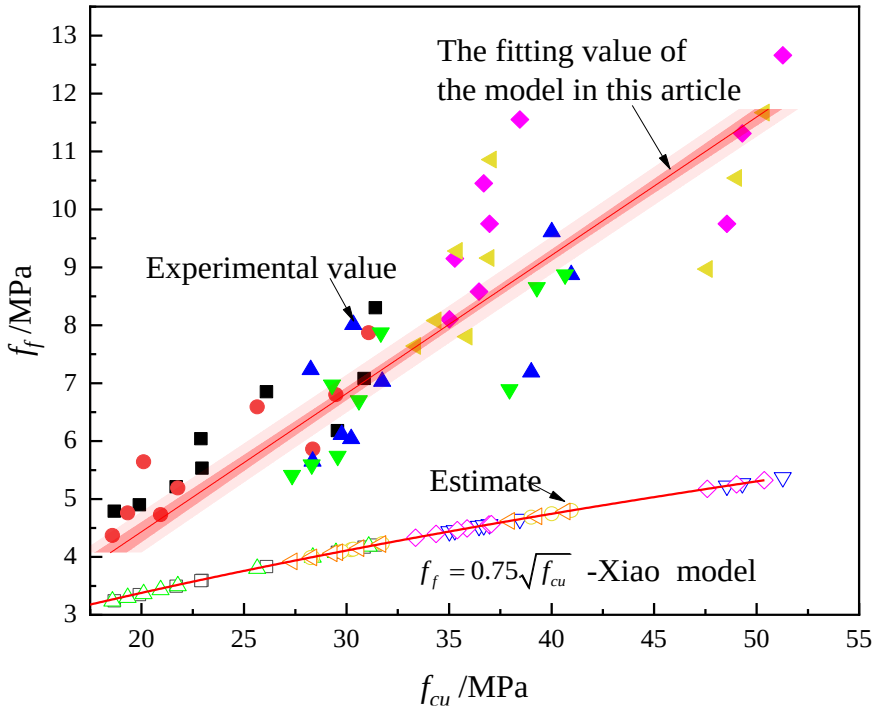


Figure 10. Prediction accuracy of flexural strength of graded EPS–steel fiber-reinforced concrete.

4. Conclusions

In this study, we analyzed the effects of different EPS and steel fiber dosages on the mechanical properties of graded EPS–steel fiber concrete made with gravel and crushed stone of different grades, through compressive and flexural strength tests. The main conclusions are as follows:

(1) **Failure Modes and Ductility**: Graded EPS–steel fiber fine aggregate and pebble concrete across different strength grades exhibited similar failure modes under compressive and flexural loading. The incorporation of graded EPS significantly enhanced ductility under compression, with the optimal ductility observed at an EPS volume fraction of 25%. Steel fibers improved ductility under flexural failure, with the best performance achieved at a volume fraction of 2.25%.

(2) **Compressive Strength**: A negative correlation was observed between the volume fraction of graded EPS and the compressive strength of concrete. The rate of strength reduction was more pronounced in the 15–25% range compared with the 25–35% range. This trend was consistent across fine aggregate and pebble concrete groups for all strength grades. Additionally, the uniaxial compressive strength at 7 days reached 60–75% of the strength at 28 days, highlighting the importance of early curing.

(3) **Workability**: an increase in the volume fraction of graded EPS significantly reduced the workability of concrete, with the slump reduction showing an accelerating trend as the EPS content increased.

(4) **Tensile Failure and Flexural Strength**: The tensile failure process of graded EPS–steel fiber concrete can be divided into four stages. Each 0.25% increase in steel fiber volume fraction resulted in a flexural strength improvement of 14.35–17.61%, with a maximum growth rate of approximately 27%. The distribution of the growth rates was relatively dispersed.

(5) **Strength Relationship and Predictive Model:** A conversion relationship between compressive strength and flexural strength was established using a correction equation incorporating the flexural-to-compressive strength ratio coefficient. The model achieved a high correlation coefficient (R) of 0.989, demonstrating strong predictive accuracy. A

method was also proposed for determining the maximum flexural-to-compressive strength ratio under the combined influence of graded EPS and steel fibers, providing valuable guidance for material design optimization.

Author Contributions: Conceptualization, Y.W. and X.Z.; methodology, Y.W.; software, Y.W.; formal analysis, Y.W. All authors have read and agreed to the published version of the manuscript.

Funding: The authors appreciate the funding from the National Natural Science Foundation of China (Grant Nos. 51978248).

Institutional Review Board Statement: Not applicable.

Informed Consent Statement: Not applicable.

Data Availability Statement: The data that support the findings of this study are available from the corresponding author upon reasonable request. The data are not publicly available due to privacy.

Conflicts of Interest: The authors declare no competing interests.

Nomenclature

α_a, α_b	Regression coefficient
σ	Standard deviation of compressive strength of concrete cube
β_s	Sand rate
m_{co}	Quality fraction of cement
m_{wo}	Quality score of water
m_{so}	Quality fraction of coarse aggregate
m_{go}	Quality fraction of fine aggregate
δ	Concrete density correction factor
W/C	Water–cement ratio

References

1. Zhang, W.H.; Lv, Y.J.; Liu, P.Y. Review on the research progress of EPS concrete. *Mater. Rev.* **2019**, *33*, 2214–2228.
2. Cardinale, T.; D'Amato, M.; Sulla, R.; Cardinale, N. Mechanical and physical characterization of papercrete as new eco-friendly construction material. *Appl. Sci.* **2021**, *11*, 1011. [CrossRef]
3. Scioti, A.; Fatiguso, F. Performance characterization and evaluation of innovative cement mortars and concretes made with recycled EPS. *Appl. Sci.* **2024**, *14*, 1583. [CrossRef]
4. Subhani, K.; Prasad, K.; Hameed, N.; Nikzad, M.; Salim, N.V. Expanded polystyrene/tyre crumbs composites as promising aggregates in mortar and concrete. *Polymers* **2024**, *16*, 3207. [CrossRef] [PubMed]
5. Qu, L.L.; Zhang, D.W. Rheological properties and corrosion resistance analysis of recycled EPS plastic/concrete composites. *Plast. Sci. Technol.* **2022**, *50*, 31–35.
6. Li, J.H.; Tian, Z.J.; Tang, T.Y.; Wang, J.D.; Zheng, Y.B.; Liu, Y.P. Influence of spherical SAP aggregate and EPS aggregate combination on the mechanical properties of concrete. *Concrete* **2021**, *4*, 70–73.
7. Zhao, D.L.; Hu, C.Y.; Bai, D.S. Current status and development trends of building energy-saving technologies in China. *Build Energy Effic* **2015**, *43*, 116–121.
8. Srinivas, K.; Akula, K.R.; Mahesh, V. Experimental investigation on lightweight concrete by replacing coarse aggregate with coconut shell and expanded polystyrene beads and using polypropylene fiber. *Mater. Today Proc.* **2021**, *46*, 838–842. [CrossRef]
9. Ferrándiz-Mas, V.; Bond, T.; García-Alcocel, E.; Cheeseman, C.R. Lightweight mortars containing expanded polystyrene and paper sludge ash. *Constr. Build. Mater.* **2014**, *61*, 285–292. [CrossRef]
10. Patricia, F.B.B.; Carmeane, E.; Adilson, S. Lightweight thermal insulating coating mortars with aerogel, EPS, and vermiculite for energy conservation in buildings. *Cem. Concr. Compos.* **2022**, *125*, 104283.
11. Yu, Z.P.; Yang, W.J.; Huang, D.K. Effect of fiber on the mechanical properties of polystyrene particle concrete. *Concrete* **2022**, *2022*, 68–72+76.
12. Luo, G.Y.; Xu, G.H.; Ren, X.; Deng, W.B.; Chen, Z.W.; Liu, C.Q. Influence of Phosphogypsum on the Carbonation and Permeability Resistance of Basalt Fiber-Reinforced Concrete. *Bull. Chin. Ceram. Soc.* **2025**, *44*, 231–242.
13. Tong, W.G.; Fan, Y.B.; Wang, H.L. Mechanical Properties of Steel-Polyvinyl Alcohol (PVA) Hybrid Fiber-Reinforced Concrete. *Concrete* **2022**, 86–88. [CrossRef]

14. Wang, Z.H.; Bai, E.L.; Ren, B.; Liu, C.J.; Zhou, J.P. Mechanical Properties of Graphene Oxide-Grafted Carbon Fiber-Reinforced Concrete. *J. Compos. Mater.* **2024**, *41*, 5504–5515.
15. Li, Q.R.; Wei, T.; Liu, K.N. Compressive constitutive model and bending toughness test of steel fiber reinforced recycled concrete. *Concrete* **2021**, *2021*, 31–35.
16. Gao, D.Y.; Zhao, L.P.; Feng, H.; Zhao, S.B. Flexural toughness of steel fiber reinforced concrete and its evaluation method. *J. Build. Mater.* **2014**, *17*, 783–789.
17. Cook, D.J. Expanded polystyrene beads as lightweight aggregate for concrete. *Precast Concr.* **1973**, *4*, 691–693.
18. Shu, X.; Zhang, Y. Stress-strain curve testing of epoxy resin/rubber concrete. *J. Wuhan Univ. Technol. (Transp. Sci. Eng. Ed.)* **2016**, *40*, 110–113+120.
19. Luo, T.T.; Liu, W.S.; Guo, Y.J. Review on the application of recycled polystyrene in concrete. *Bull. Chin. Ceram. Soc.* **2021**, *40*, 133–145.
20. Liu, Y.C.; Zhang, L.X.; Zhan, J.P.; Cai, Y.C. Strength model of EPS lightweight concrete. *Concrete* **2013**, *36–37*, 45.
21. Zhou, K.K.; Chen, B.; Chen, L.Z. Effect of EPS particle gradation on the mechanical properties of EPS concrete. *J. Harbin Eng. Univ.* **2010**, *31*, 195–201.
22. Yang, Y.M.; Ge, Z.S. Impact test study on the full lightweight concrete beams with different steel fiber contents. *Build. Struct.* **2024**, *54*, 59–64.
23. Wu, D.Y.; Yao, Q.S.; Diao, F.; Wang, F.; Man, H.W. Flexural toughness and impact resistance of steel fiber reinforced recycled concrete. *Concrete* **2023**, *22*, 141–144.
24. Anjaney, A.; Dix, I.T.; Sung, H.K. Lightweight structural cement composites with expanded polystyrene (EPS) for enhanced thermal insulation. *Cem. Concr. Compos.* **2019**, *102*, 185–197.
25. *GB/T14902–2012*; Pre-Mixed Concrete. China Standard Press: Beijing, China, 2013.
26. *GB/T 50081–2019*; Standard for Physical and Mechanical Property Testing Methods of Concrete. China Building Industry Press: Beijing, China, 2019.
27. *CECS 13–2009*; Test Method Standards for Fiber Concrete. China Planning Press: Beijing, China, 2010.
28. Zhang, X.N.; Guo, Z.X.; Wu, K.H. Design of asphalt mixtures by volume method. *J. Harbin Univ. Archit.* **1995**, *1995*, 28–36.
29. *GB/T 50080–2002*; Standard for Performance Test Methods of Common Concrete Mixes. China Building Industry Press: Beijing, China, 2002.
30. Pan, W.L.; Deng, D.H.; Yuan, T.P.; Zeng, Z. Influence of EPS lightweight concrete mix ratio on its fluidity and mechanical properties. *Concrete* **2006**, *63–65*, 69.
31. *JTG D40–2002*; Specification for Highway Cement Concrete Pavement Design. Ministry of Transport of the People's Republic of China: Beijing, China, 2002.
32. Xiao, J.Z.; Lin, Z.B.; Zhu, J. Effect of recycled aggregate gradation on the compressive strength of concrete. *J. Sichuan Univ. (Eng. Sci. Ed.)* **2014**, *46*, 154–160.
33. Zhang, X.G.; Kuang, X.M.; Zhang, X.X.; Deng, D.P.; Yang, J.H. Study on the conversion relationship between flexural and compressive strength of semi-lightweight shale aggregate concrete. *Bull. Silic.* **2018**, 2264–2269.

Disclaimer/Publisher's Note: The statements, opinions and data contained in all publications are solely those of the individual author(s) and contributor(s) and not of MDPI and/or the editor(s). MDPI and/or the editor(s) disclaim responsibility for any injury to people or property resulting from any ideas, methods, instructions or products referred to in the content.